Air Cooling Enhancement in Entrance Region with Delta Winglet Vortex Generators Set at the First Row of In-Line Array of Electronic Module

Suriyon Chomdee and Tanongkiat Kiatsiriroat*

Department of Mechanical Engineering, Faculty of Engineering, Chiang Mai University, Chiang Mai 50200, Thailand

**Corresponding author. E-mail: tanong@dome.eng.cmu.ac.th*

ABSTRACT

The objective of this study was to experimentally investigate the heat transfer enhancement by delta winglet vortex generators for air cooling in entrance region of in-line array of electronic modules. The study had been carried out when the winglet pairs were placed in front of the first row of the array. Each module had a dimension of 1.8 cm x 5.8 cm x 0.6 cm and each one generated heat at 5 W. The adiabatic heat transfer coefficients and the thermal wake for the modules with and without the generators were considered at different values of Reynolds number. It was evident that the vortex generators could enhance the adiabatic heat transfer coefficients, reduce the thermal wake function and the module temperature, especially for the first row. Moreover, the correlations to predict the heat transfer data had been developed when the vortex generators were integrated and the predicted module temperatures agreed very well with those of the experiments.

Key words: Electronic cooling, Vortex generator, Heat transfer enhancement

INTRODUCTION

There are many techniques for the thermal management but the convective air cooling is still the most common for electronic cooling because of its low maintenance and low investment cost. However, the common forced-air cooling is not sufficient in case of high power dissipation, especially, for the complex electronic components.

Heat transfer enhancement of air cooling by vortex generator is one passive method that generates streamwise vortices which creates high turbulence in fluid flow over heat transfer surfaces. Delta winglet vortex generator is one of the promising techniques to integrate in compact heat exchangers and shows a very good heat transfer performance. There was a report (Wrobleski and Eibeck, 1991) which showed that the longitudinal vortices imbedded into turbulent boudary layers could enhance the heat transfer. Some researchers (Fiebig et al., 1986, 1993; Fiebig, 1998) had studied the influences of different types of vortex generators on heat transfer performance such as delta wing, rectangular winglet and delta winglet and the best performance was found in the delta winglet type.

Vortex generators have also been applied to enhance heat transfer in electronic modules. There was a report (Garimella and Eibeck, 1991) which investigated heat transfer enhancement by installing a row of half-delta wing vortex generators upstream of a heated copper chip array. The study used water as a coolant and two heights of the vortex generators (one and two times of the chip's height).

Thermal wake and pressure drop characteristics in a set of electronic modules when there were different shapes and sizes of ribs fixed to the array board had also been studied (Jubran and Al-Saleymeh, 1999). The thermal wake function of the chips downstream could

be reduced significantly.

The present study aimed to experimentally investigate the entrance heat transfer performance of in-line electronic module array with the presence of delta winglet vortex generators integrated in front of the first row of the array.

EXPERIMENTAL PROCEDURE

The experiments were performed in a small wind turbine with a test section as shown in Figure 1. The air flow rate could be controlled and the height of the air channel could be adjusted. There was a flow straightener to keep the uniform airflow before entering the test section.

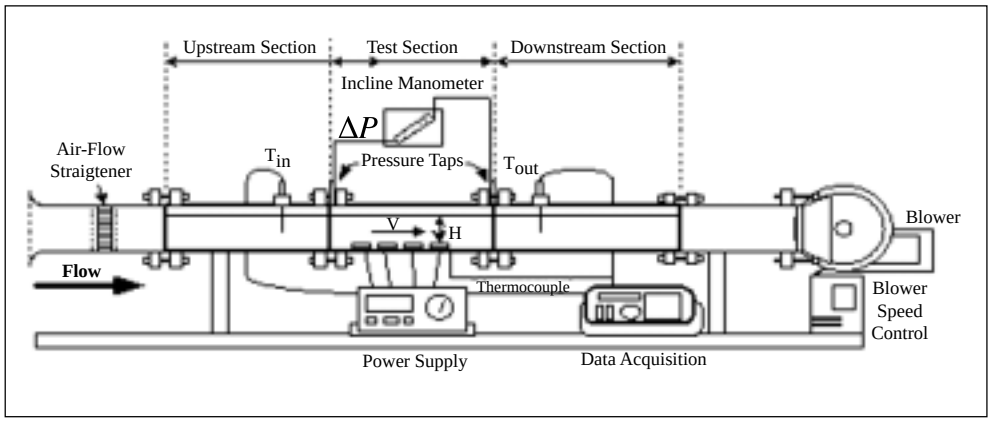

Figure 1. The experimental setup.

The modules of the study were artificial elements, each of 1.8 cm x 5.8 cm x 0.6 cm, having a 5 W electrical foil-heater inside. The module dimensions were similar to those of the real 64 pin electronic chip and they were attached on an epoxy board. Each artificial module was polished aluminum and because of its high thermal conductivity, the radiation effect could then be neglected (Rodgers et al., 2003). Between the module and an epoxy board there was an insulator tape and the epoxy board was also insulated at the back, thus the heat conduction to the board was rather small. The modules were arranged in 4 in-line rows, each contained 4 elements. The delta winglet vortex generators were also integrated into the board as shown in Figure 2. The temperatures of the chips and the inlet air temperature were measured by a set of K-type thermocouples having ±1°C accuracy, the rate of heat generated in each chip was read directly from a wattmeter with ±0.1 W accuracy and the air inlet velocity was monitored by a hot-wire anemometer with ±0.1 m/s accuracy. The data at steady-state conditions are used to derive the heat transfer coefficients and the thermal wake function. The experimental test conditions are given in Table 1.

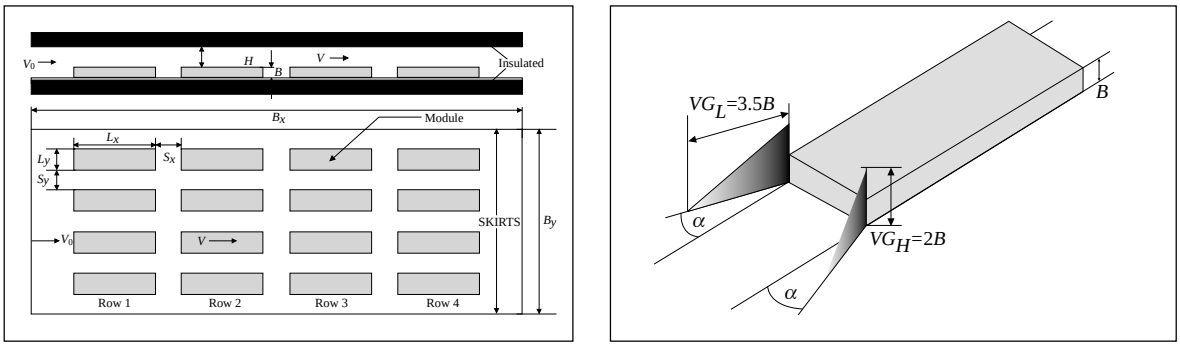

Figure 2. The chip module array and the vortex generator.

Table 1. The test conditions.

variables	values
Re_H	3600/5400/7200/9000
H	0.018 m.
B	0.006 m.
L_X	0.058 m.
L_Y	0.018 m.
S_X	0.019 m.
S_Y	0.018 m.
B_X	0.420 m.
B_Y	0.160 m.
VG_H	0.012 m.
VG_L	0.021 m.
α	20 degree
q_k	5 Watt/module
$k_{(PCB),\ Epoxy}$	2 W/m°K
T_0	27°C

DATA REDUCTION

The temperature rise in electronic module, for convective effect, comes from its heat generation and thermal wake which results in heat release from the upstream components.

When the thermal radiation effect is neglected, the temperature rise in each electronic chip can be calculated by (Arvisu and Moffat, 1982)

$$T_k - T_0 = \left(\frac{q_k}{h_k A_k}\right) + \sum_{i=1}^{k-1} \theta_{k\text{-}i}\,(T_i - T_0),\ i < k\ . \qquad (1)$$

q_k is the internal heat generation in the k^{th} chip, A_k is the heat transfer area and h_k is adiabatic heat transfer coefficient which can be calculated from

$$h_k = \frac{q_k}{A_k (T_k - T_0)} \Big| only\ q_k \ \ 0. \tag{2}$$

θ_k is thermal wake function which is the fraction temperature increase of the k^{th} component due to heat release from the other elements. The function can be calculated by

$$\theta_{k-i} = \frac{T_k - T_0}{T_i - T_0} \Big| q_i \quad 0,\ q_k = 0. \tag{3}$$

RESULTS

Adiabatic Heat Transfer Coefficient

(a) No vortex generator

Figure 3 shows the adiabatic heat transfer coefficient in terms of Nusselt number at different positions when there was no vortex generator. The results of the first to the third row which were in the entrance region were similar to those of other researchers (Anderson and Moffat, 1990).

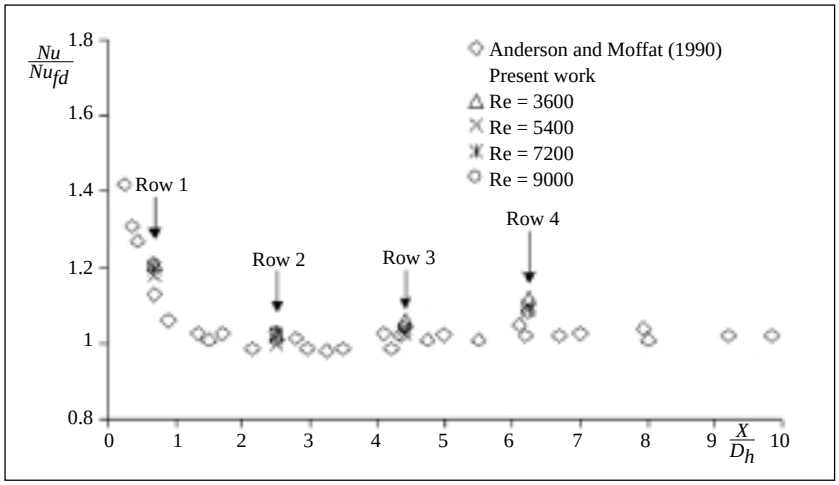

Figure 3. The ratio of adiabatic Nusselt number at different postitions to that at the first row at various values of x/D_h. No vortex generator.

From Figure 3 the Nusselt number can be set in a form as

$$\frac{Nu}{Nu_{fd}} = 1 + 0.0786 \left(\frac{X}{D_h} \right)^{-1.099} . \tag{4}$$

where

$$\mathrm{Nu}_{fd} = 0.3434\mathrm{Re}_H^{0.607}\left(\frac{H}{L_X}\right)^{-0.670}\left(\frac{S_X}{L_X}\right)^{0.295} \quad (5)$$

It can be seen that the second row got the poorest heat transfer coefficient, followed by the third row because there was a recirculation perpendicular to the secondary air flow existing in the inter-block gaps. The last-chip heat transfer coefficient was higher than those of the second and the third elements because the air could move more freely.

Figure 4 also shows the value of the Nusselt number at various positions compared with that at the first row when there was no vortex generator.

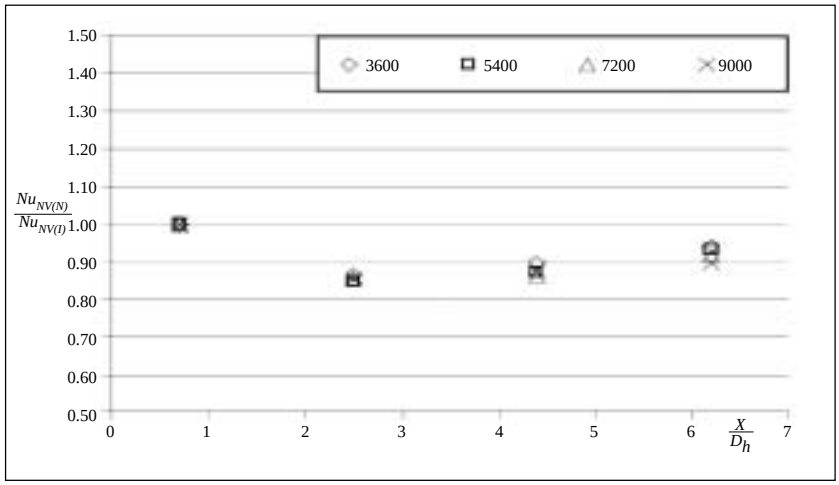

Figure 4. The ratio of adiabatic Nusselt number at different positions to that at the first row at various values of $\frac{X}{D_h}$. No vortex generator.

From the figure, it can be seen that the value of Reynolds number slightly affects the ratio of the Nusselt number at different positions to that at the first row. For the entrance region (row 1 to row 3), a correlation can be performed as

$$\frac{Nu_{(NV)(N)}}{Nu_{NV(1)}} = 0.82959\mathrm{Re}_H^{-0.0122919}\left(\frac{X}{D_h}\right)^{-0.081162} . \quad (6)$$

The correlation gives ± 6% error from the experimental data.

(b) With vortex generators

When a set of vortex generators were installed only in front of the first row, the chip modules at the first row got a strong effect of the longitudinal flow, thus high heat transfer enhancement was obtained as shown in Figure 5. The vortex generators also enhanced the heat transfer in the next rows. It could also be found that the Reynolds number did not give the strong effect on the heat transfer enhancement.

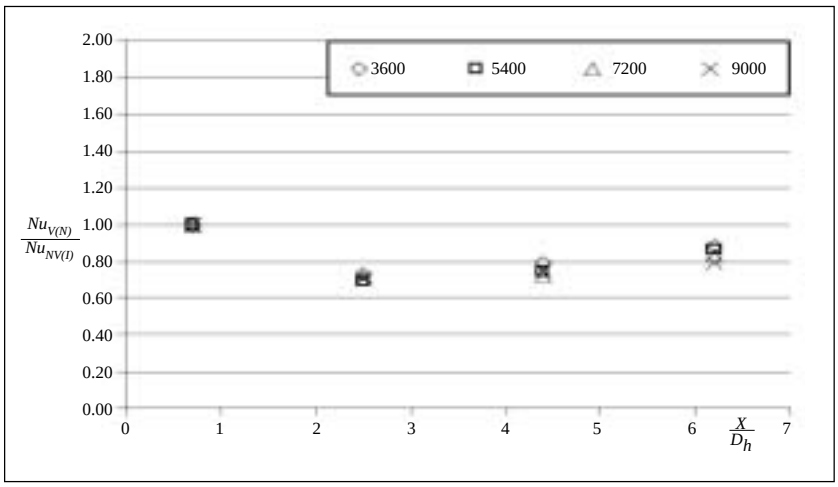

Figure 5. The heat transfer enhancement in terms of adiabatic Nusselt numbers with and without vortex generators. The vortex generators were integrated in front of the first row only. The attack angle was 20 degree.

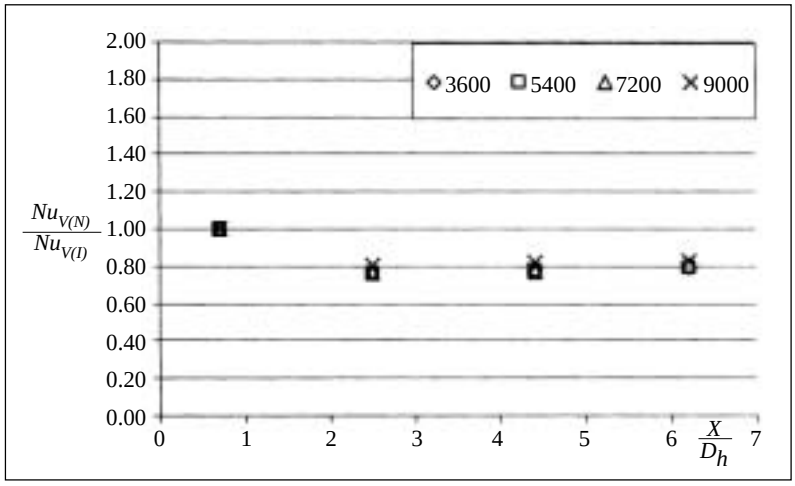

Figure 6. The ratio of adiabatic Nusselt number at different postitions to that at the first row at various values of $\frac{X}{D_h}$ and different attack angles. There was a set of vorte generators integrated in front of the first row only.

Figure 6 also shows the ratio of adiabatic Nusselt number at different positions at 20° attack angle with that at the first row when there was a set of vortex generators at the first row and the parameters related can be correlated as

$$\frac{Nu_{V(N)}}{Nu_{V(1)}} = 0.46392\mathrm{Re}^{-0.027878}\left(\frac{X}{D_h}\right)^{-0.14385} . \quad (7)$$

The correlation gives ± 9% error from the experimental data.

To generate a relation between the heat transfer data of the modules with and without the vortex generators, a correlation between the Nusselt numbers in the first row and the Reynolds number is given as

$$\frac{Nu_{V(1)}}{Nu_{NV(1)}} = 1.6588\mathrm{Re}^{-0.0402} . \quad (8)$$

The correlation gives ± 2% from the experimental data. The results are also given in Figure 7.

From the above correlations, the adiabatic Nusselt number of the modules with integrated vortex generators can be evaluated from that without the vortex generator as

$$\frac{Nu_{V(N)}}{Nu_{NV(N)}} = \left(\frac{Nu_{V(N)}}{Nu_{V(1)}}\right) \text{x} \left(\frac{Nu_{V(1)}}{Nu_{NV(1)}}\right) \text{x} \left(\frac{Nu_{NV(1)}}{Nu_{NV(N)}}\right) . \quad (9)$$

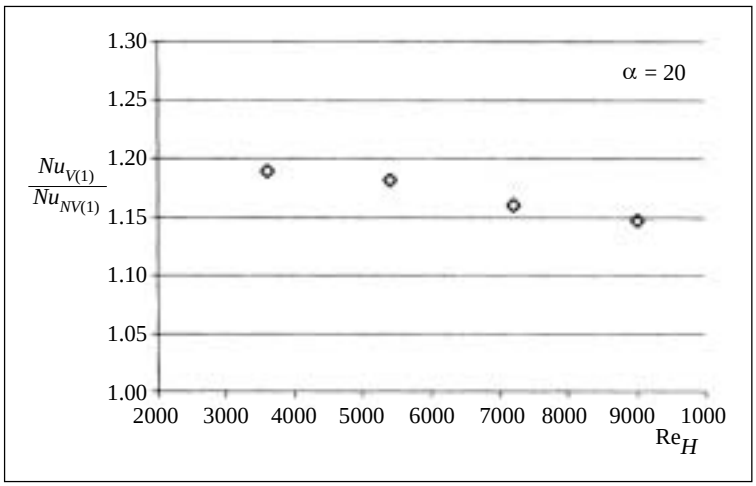

Figure 7. The ratio of the adiabatic Nusselt numbers of the first row with and without vortex generators. The vortex generators were integrated only in front of the first row.

Thermal Wake Function

(a) No vortex generator

When one row of electronic modules is heated, the temperatures of the modules downstream will also get this heating result which is called the thermal wake effect. Figure 8 shows the results of thermal wake function of the module immediately downstream from the first heating module when there was no vortex generator. Figure 9 shows the thermal wake functions for other downstream modules. It can be seen that the thermal wake functions of the modules are similar to that described by other researchers (Faghri et al., 1996; Jubran and Al-Saleymeh, 1999) of which the correlations of the thermal wake functions are

$$\frac{\theta_{NV(N)}}{\theta_{NV(1)}} = 0.20756 Re_H^{0.17935} N^{-0.76936} , \quad (10)$$

where

$$\theta_{NV(1)} = 4.9065 Re_H^{-0.3571} . \quad (11)$$

The correlation gives ± 10% from the experimental data. An example of the calculation at $Re_H = 5400$ compared to the literature data (Jubran and Al-Saleymeh, 1999) is also shown in Figure 10.

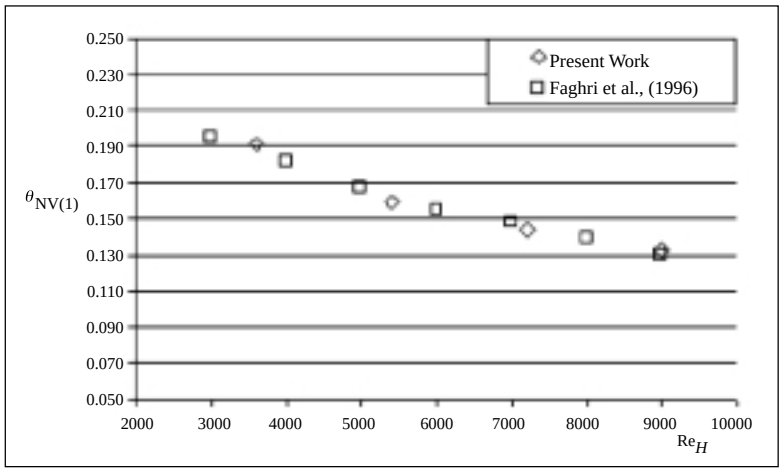

Figure 8. Thermal wake function for the first adiabatic module. No vortex generator.

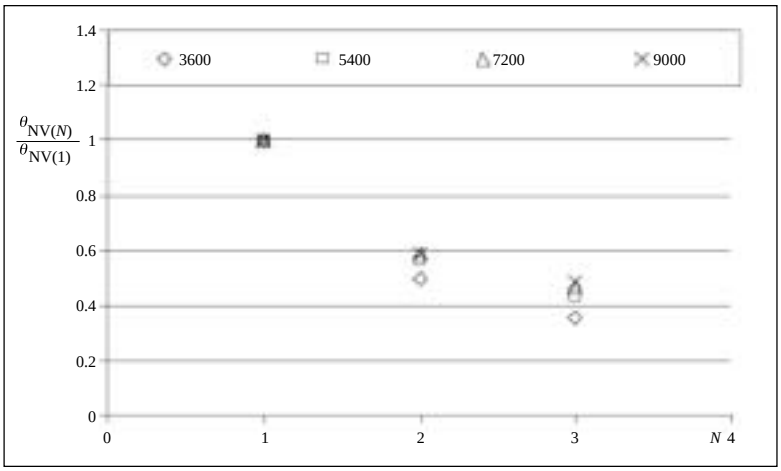

Figure 9. The thermal wake functions for other downstream modules. No vortex generator.

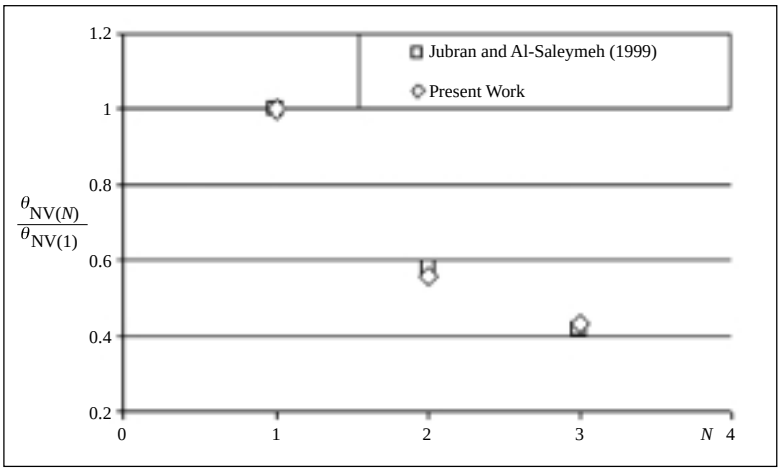

Figure 10. The thermal wake functions for other downstream modules compared with the data of Jubran and Al-Saleymeh (1999). No vortex generator.

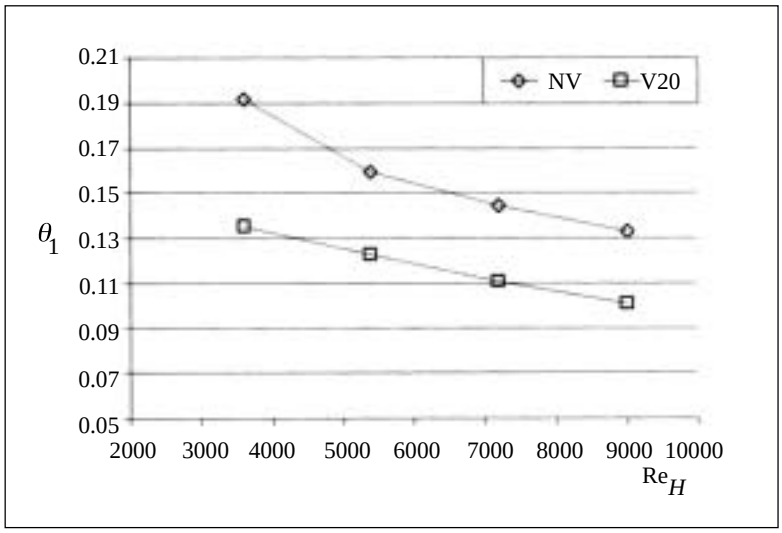

Figure 11. Thermal wake function for the first adiabatic module. Vortex generators were integrated in front of the first row.

(b) With vortex generators

Figures 11 shows the thermal wake functions of the modules when there was a set of vortex generators in front of the first row. It can be seen that the technique could reduce the thermal wake function effectively due to the longitudinal vortex promotion by the vortex generators. Figure 12 also gives the ratio of the thermal wake functions for other downstream modules to that of the first row.

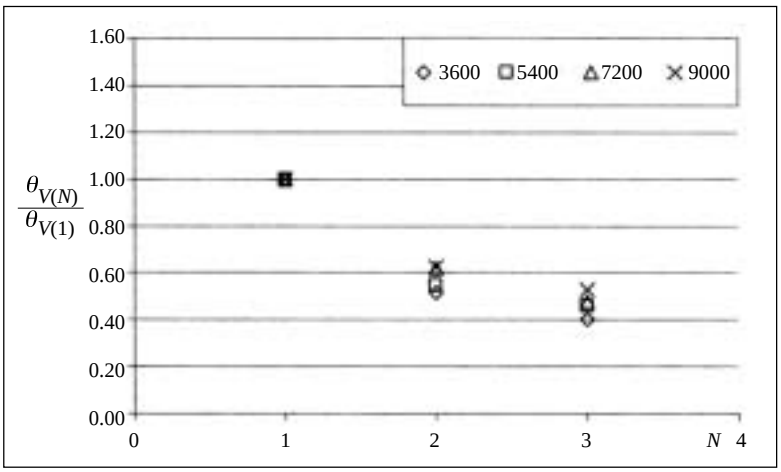

Figure 12. The thermal wake functions for other downstream modules. Vortex generators were integrated in front of the first row.

A correlation of the thermal wake function with the related parameters can be written in a form as

$$\frac{\theta_{NV(N)}}{\theta_{V(1)}} = 0.22506 \mathrm{Re}_H^{0.1697} N^{-0.71125} \quad . \tag{12}$$

The correlation gives ± 10% error from the experimental data.

Similarly, to relate the equation of the modules having a set of vortex generators to that without the generators, a correlation of the thermal wake functions in the first row can be written in a form as

$$\frac{\theta_{V(1)}}{\theta_{NV(1)}} = 0.0156\mathrm{Re}_H^{0.4236} \quad . \tag{13}$$

The correlation gives ± 8% error from the experimental data. The results are also shown in Figure 13.

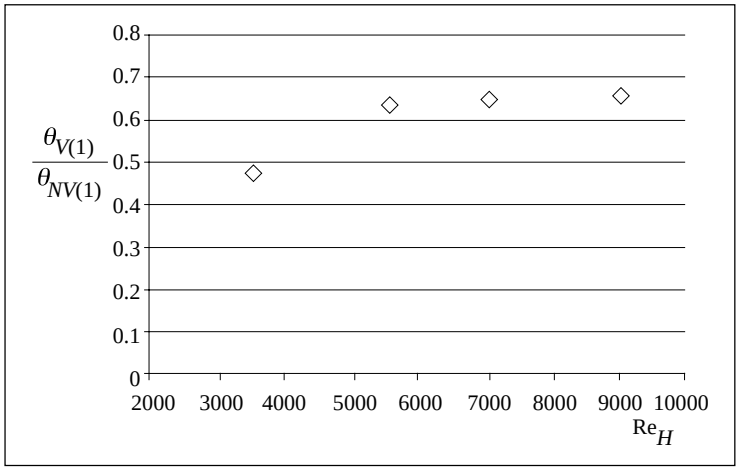

Figure 13. The ratio of thermal wake functions of the modules with and without vortex generator at the first row.

The thermal wake function of the modules with integrated vortex generators can be evaluated from that without the vortex generator as

$$\frac{\theta_{V(N)}}{\theta_{NV(N)}} = \left(\frac{\theta_{V(N)}}{\theta_{V(1)}}\right) \mathrm{x} \left(\frac{\theta_{V(1)}}{\theta_{NV(1)}}\right) \mathrm{x} \left(\frac{\theta_{NV(1)}}{\theta_{NV(N)}}\right) \quad . \tag{14}$$

Module Temperatures

Figure 14 shows the module temperatures when the vortex generators were integrated at the first row of the module array. It could be seen that when the array was integrated with vortex generators, the module temperatures were lower than those without the devices. The calculated results of the module temperatures from the technique described agreed very well with those of the measured data.

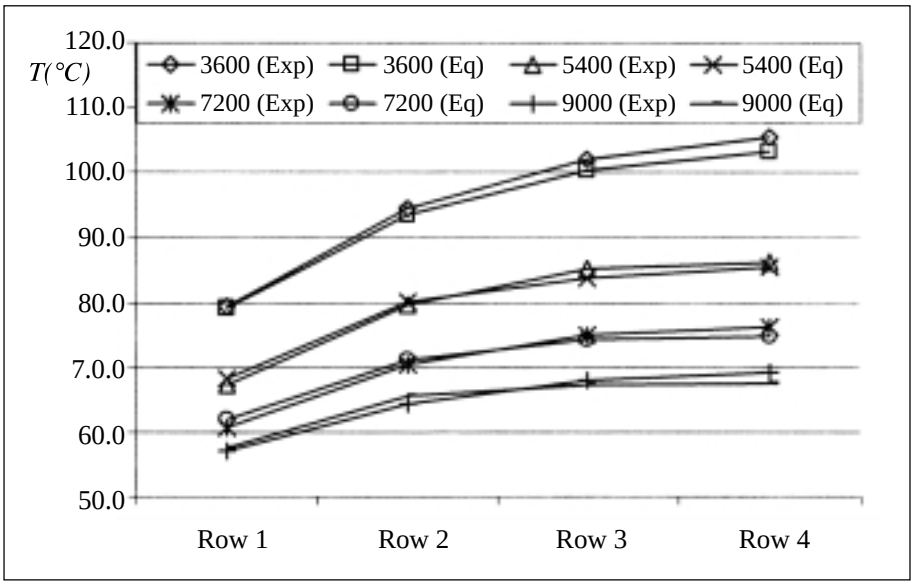

Figure 14. The module temperatures when the vortex generators were integrated.

Pressure Drop

The pressure drop of air flow in the channel having the electronic modules with and without vortex generators was found to be nearly the same. The results are shown in Figure 15.

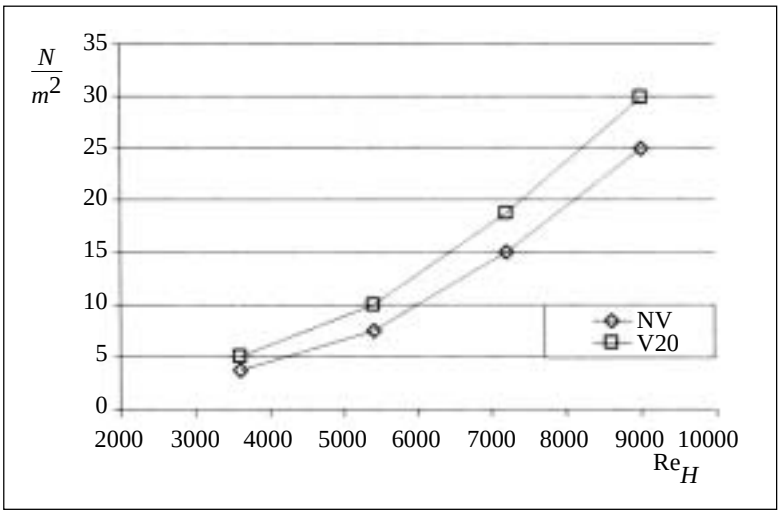

Figure 15. Pressure drop in air flow.

CONCLUSION

From this study, it can be concluded that

1. The vortex generators could enhance the heat transfer significantly for the modules in the first row.
2. The pressure drop in air flow when the vortex generators were included was very close to that without the generators.
3. The method developed could be used to predict the module temperature very well.

ACKNOWLEDGEMENTS

The authors would like to express gratitude to the Thailand Research Fund for supporting this research work.

REFERENCES

Anderson, A.M., and R. J. Moffat. 1990. A new type of heat transfer correlation for air cooling of regular arrays of electronic components. Proc. ASME Annual. Meet.27–39.

Arvizu, D. E., and R. J. Moffat. 1982. The use of superposition in calculating cooling requirements for circuit board mounted electronic components. IEEE paper CH1781–4/ 48–0133.

Faghri, M., M. Molki, and Y. Asako. 1996. Entrance design correlations for circuit boards in forced-air cooling. p. 47–80. In J. K. Sung and W. L. Sang(eds) Air cooling technology for electronic equipment. CRC Press.

Fiebig, M., P. Kallweit, and N. K. Mitra. 1986. Wing-type vortex generators for heat transfer enhancement. Proceeding of the 8th Int. Heat Transfer Conference, San Francisco 6 : 2909–2913.

Fiebig, M. 1998. Vortices, generators and heat transfer. Trans.IChemE76 (Part A). 108–123.

Fiebig, M., A. Valencia, and N. K. Mitra. 1993. Wing-type vortex generators for fin-and- tube heat exchangers, Exp. Thermal Fluid Sci. 7 : 287–295.

Garimella, S. V., and P.A. Eibeck. 1991. Enhancement of single phase convective heat transfer from protruding elements using vortex generators. Int. J. Heat Mass Transfer 34(9) : 2431–2433.

Jubran, B. A., and A.S. Al-Saleymeh. 1999. Thermal wakes measurement in electronic modules in the presence of heat transfer enhancement devices. Applied Thermal Engineering 19 : 1081–1096.

Rodgers, P. J., V. C. Eveloy, and M. R. D. Davies. 2003. An experimental assessment of numerical predictive accuracy for electronic component heat transfer in forced convection- Part 1: Experimental methods and numerical modeling. ASME J. Electronic Packaging 125 : 67–75.

Wirtz, R.A. 1996. Forced-air cooling of low-profile package arrays. p. 81–95. In J. K. Sung and W. L. Sang(eds) Air cooling technology for electronic equipment. CRC Press.

Wrobleski, D.E., and P. A. Eibeck. 1991. Measurements of the turbulent heat transport in a boundary layer with an embedded streamwise vortex. Int. J. Heat Mass Transfer 34 : 1617–1631.

NOMENCLATURES

A_k surface area of the chip module, m^2

B module height, m

B_X length of PCB, m

B_y width of PCB, m

D_h hydraulic diameter $\left(\frac{2W(H+B)}{(W+H+B)}\right)$

h_k heat transfer coefficient, $\frac{W}{m^2°C}$

H space between the module and the opposite wall of the air channel, m

k_{PCB} thermal conductivity of PCB, $\frac{W}{m°C}$

L_X module length, *m*
L_y module width, *m*
N adiabatic block situated downstream of the heated block
Nu Nusselt number $\left(\frac{h_k L_x}{k}\right)$
q_k heat generated from the kth module, *W*
Re_H Reynolds number, $\left(\frac{VL_x}{\nu}\right)$
S_X module spacing in X direction, *m*
S_Y module spacing in Y direction, *m*
T_i temperature of the module before the considered one, °*C*
T_K temperature of the considered module, °*C*
T_0 inlet air temperature, °*C*
V_0 inlet air velocity, (*m/s*)
V air velocity over the module, (*m/s*)
VG_H height of vortex generator, *m*
VG_L length of vortex generator, *m*
X length from the leading edge of the first module, *m*
θ thermal wake function
α attack angle

Suffices

V(1) with vortex (row 1)
NV(1) no vortex (row 1)
V(N) with vortex (row N)
NV(N) no vortex (row N)
fd fully developed flow